ALPHONSUS CRATER: INFLUENCE OF TOPOGRAPHY ON ERUPTION DYNAMICS AND MINERAL DISTRIBUTION. L.M. Glaspie[1], L.R. Gaddis[2], L. Keszthelyi[2], M. Hunter[2], J. Laura[2], B. Horgan[3], J. Stopar[3], S. Lawrence[4], M.P. Milazzo[2]. [1]Dept. of Physics & Astronomy, Northern Arizona University, Flagstaff, AZ. [2]Astrogeology Science Center, U.S. Geological Survey, Flagstaff, AZ 86001. [3]Purdue University, W. Lafayette, IN. [3]Lunar & Planetary Institute, Houston, TX. [4]NASA Johnson Space Center, Houston, TX. (lglaspie@usgs.gov)

Introduction: Alphonsus crater (13°S, 357°E; 108 km dia.) is a Lower Imbrian-aged crater with multiple localized crater-floor, endogenic "dark halo" deposits [1]. Here we characterize the eruption of one dark halo crater within Alphonsus, Alphonsus R (~2.7 km dia., [2]; ***Figure 1***) based on high-resolution images, derived topographic products, and eruption modeling. We do this by visualizing the composition and spatial distribution of materials on a 3-dimensional topographic projection and by modeling the eruption. The objective is to assess the influence of local topography on the eruption and to constrain the eruption style, volatility and duration. Previous studies [3,4] eliminated topography as a variable in analyzing composition to simplify their modeling analyses. In addition to providing the first analysis of the effect of topography on composition and distribution of pyroclastic materials, this study will inform future studies of composition overlaid on topographic models in 3D and provide a better baseline with which to confirm the validity and accuracy of such modeling.

Background: Head and Wilson [2] interpreted "dark halo" deposits such as those at Alphonsus R as likely resulting from conditions typified by Vulcanian eruption activity followed by fire fountaining. Using hyperspectral data from the NASA Moon Mineralogy Mapper (M^3) instrument on the ISRO Chandarayaan-1 spacecraft [5], Gaddis et al. [6] studied individual vent sources within the floor of greater Alphonsus crater. Craters within Alphonsus are interpreted as pyroclastic when characterized with the association of dark mantling, non-circular outline, mafic mineralogy, and positive-relief features. The compositions of Alphonsus R dark-halo deposits indicate a mixture of volcanic glass, clinopyroxene, and orthopyroxene [6].

Geologic Analysis: *Regional Geology of Alphonsus and Alphonsus R.* Alphonsus crater is located in the highlands east of Mare Nubium and has a broad, low rim with a central ridge (running approximately north-south) and a central peak. The generally flat cratered floor of Alphonsus is dissected by numerous floor fractures, around which Alphonsus R and 10 other pyroclastic vents and deposits are located [6]. This association indicates that the fractures are likely reservoirs for volatile accumulation and provided a locus for pyroclastic eruption. Head and Wilson [2] estimated that Alphonsus pyroclastic deposits comprise ~50% juvenile and ~50% non-juvenile material. Recent studies with M^3 data indicate that iron-rich volcanic glass is present in all Alphonsus pyroclastic deposits, including Alphonsus R (***Figure 2***). Glass is most abundant near the vent [6] and generally decreases in abundance radially away from the vent.

Influence of topography on spatial distribution. The topographic influence on the distribution of volcanic glass (***Figure 2***) and mafic minerals (***Figure 3***) at Alphonsus R can be visualized in the M^3 data as it is draped over the topography and projected in 3D. A ballistic model of pyroclastic eruptions has been developed by Keszthelyi et al. [7]; initial results suggest that local, initial vent, and changing deposit topography have strongly influenced the emplacement and extent of the pyroclastic deposit. For example, at Soraya crater in the northeast floor of Alphonsus, an escarpment on the east margin appears to have limited the extent of the pyroclastic material in that direction of the eruption. Mass wasting from the escarpment onto the pyroclastic deposit also may have further truncated the extent of the pyroclastic deposit to the east.

Methods: To assess the influence of topography on pyroclastic deposit emplacement and composition at Alphonsus, we focus on Alphonsus R crater. Alphonsus R was chosen for this analysis because it is an isolated dark-halo deposit within a well-studied area with readily characterized pyroclastic features. Using M^3 global imaging mode data (140 m/pixel spatial resolution, OP1B/2A) with spectral resolution of 20-40 nm in 85 channels between 460 and 3000 nm, these data allow us to identify and map soil and rock mineralogies that can be related to their volcanic eruption and emplacement styles [6].

Compositional analysis. In using the methods described by Gaddis et al. [6, and references therein], we characterize the position and shape of the 1 and 2 μm iron absorption bands in M^3 data to identify and map mineralogy of Alphonsus crater floor. We first smooth the data and then remove the continuum, finding local band maxima near 0.7, 1.5, and 2.6 microns. The "glass band depth" spectral parameter is calculated as the average band depth below the continuum at 1.15, 1.18, and 1.20 μm, and the "orthopyroxene (OPX) band depth" spectral parameter is calculated as the average band depth below the continuum at 0.88, 0.90, and 0.92 μm. The band analysis methods of Horgan et al. [8] are then used to parameterize the centers and

depths of the 1 and 2 μm iron absorption bands. Maps of these parameters are used to distinguish between orthopyroxene (OPX; band centers between 0.9-0.94 and 1.8-1.95 μm), clinopyroxene (CPX; 0.98-1.06 and 2.05-2.4 μm), and iron-bearing glass (1.06-1.2 and 1.9-2.05 μm). Mixtures of these minerals have band centers that fall between the endmembers [8].

Observations and Interpretation. Volcanic glass is widespread throughout the Alphonsus R deposit, consistent with rapid emplacement of juvenile material. The distribution of crater-floor-like OPX away from the vent at Alphonsus R suggests an energetic initial explosion, followed by fire-fountaining to form glass-rich deposits. The near-vent CPX signatures could be thicker pyroclastic deposits, thin flows, or fragmented basalt from within the source dike.

Summary and Future Work: These data indicate that topographic and compositional information can be used together to characterize the eruption styles of pyroclastic deposits at Alphonsus and elsewhere on the Moon. Working with our simple emplacement model [7] and detailed morphologic data [9] for all of the Alphonsus deposits, we will add compositional information from the Kaguya Spectral Profiler (SP) instrument [10] to further characterize deposit mineralogy. The SP data (500 m footprint, 140 m on the lunar surface; spectral range of ~500-2500 nm through the visible and near-infrared) provide additional hyperspectral compositional data to improve surface mapping of composition. Using 3-D rendering of M^3 and SP data on the best available topographic model [11], we will study the topographic influence on the distribution of juvenile and non-juvenile materials at Alphonsus R and other deposits.

This work will allow us to characterize the location and distribution of iron-rich glass available in pyroclastic material for studies such as *in situ* resource utilization and oxygen production [12]. The erupted juvenile volcanic material (including volcanic glass and mafic minerals such as pyroxene and olivine) at Alphonsus and other lunar pyroclastic deposits may be the best samples from the lunar interior from which to extract compositional clues about the origin of the Moon and the early planetary formation environment.

References: [1] Gaddis L.R. et al. (2002) Icarus, 161, 262-280. [2] Head J.W., Wilson, L. (1979) PLPSC 10th., 2861-2897. [3] Trang et al. (2017) Icarus 283, 232-253. [4] Gustafson, J.O., et al. (2012) JGR 117. [5] Goswami & Annadurai, (2009) Curr. Sci., 96 (4), 486-491. [6] Gaddis L.R. et al. (2016) LPSC 47th, Abstract #2065. [7] Keszthelyi, L. et al. (2018) this meeting. [8] Horgan et al. (2014) Icarus, 234,(C)132-154. [9] Hunter, M. et al. (2018) this meeting. [10] Haruyama et al. (2008) *Adv. Sp. Res. 42* 310-316. [11] Barker et al. (2015) *Icarus, 273* 346-355. [12] Allen et al. (2015) *LPSC* 46th Abstract #1140.

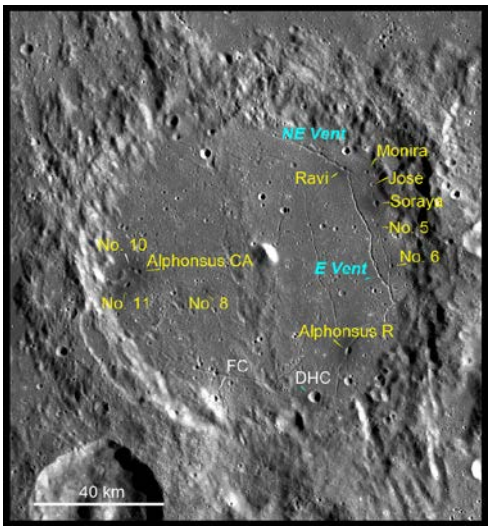

Figure 1. *Alphonsus crater: a) Kaguya Terrain Camera mosaic showing dark halo deposits, the central peak, a fresh crater (FC), and an impact-related dark-halo crater (DHC).*

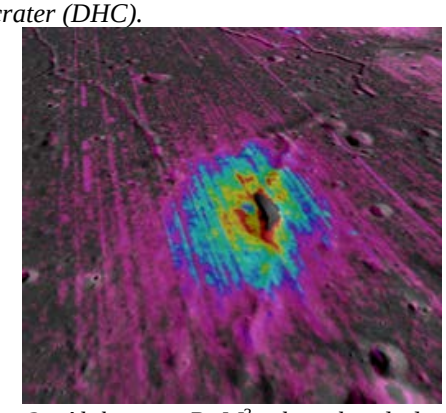

Figure 2. *Alphonsus R M^3 glass band depth data draped over topographic model [11].*

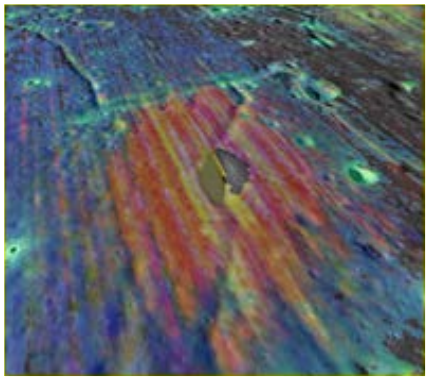

Figure 3. *Alphonsus R M^3 data draped over topographic model [11]. Blue: CPX, green: OPX, yellow: glass (G) & CPX, pink: G & OPX, teal: OPX & CPX.*